Meas. Sci. Technol. **18** (2007) 3537–3546 doi:10.1088/0957-0233/18/11/038

Cosmic ray detection based measurement systems: a preliminary study

I Bodini[1], **G Bonomi**[1,2], **D Cambiaghi**[1], **A Magalini**[1] **and A Zenoni**[1,2]

[1] Università degli Studi di Brescia, Facoltà di Ingegneria, Dipartimento di Ingegneria Meccanica ed Industriale. Via Branze, 38-25123 Brescia, Italy
[2] Istituto Nazionale di Fisica Nucleare. Via Bassi, 6-27100 Pavia, Italy

E-mail: ileana.bodini@ing.unibs.it

Received 20 March 2007, in final form 8 August 2007
Published 4 October 2007
Online at stacks.iop.org/MST/18/3537

Abstract
Cosmic rays, mostly composed of high energy muons, continuously hit the Earth's surface (at sea level the rate is about 10 000 m^{-2} min^{-1}). Various technologies are adopted for their detection and are widespread in the field of particle and nuclear physics. In this paper, cosmic ray muon detection techniques are assessed for measurement applications in engineering, where these methods could be suitable for several applications, with specific reference to situations where environmental conditions are weakly controlled and/or where the parts to be measured are hardly accessible. Since cosmic ray showering phenomena show statistical nature, the Monte Carlo technique has been adopted to numerically simulate a particular application, where a set of muon detectors are employed for alignment measurements on an industrial press. An analysis has been performed to estimate the expected measurement uncertainty and system resolution, which result to be strongly dependent on the dimensions and geometry of the set-up, on the presence of materials interposed between detectors and, ultimately, on the elapsed time available for the data taking.

Keywords: cosmic ray muons, multiple scattering, mechanical alignment monitoring, Monte Carlo simulations, elementary particle detectors, position measurements

1. Introduction

Primary cosmic rays are mainly composed of high energy protons coming from the Sun and from the outer Galaxy. When such particles enter the Earth's atmosphere, they eventually collide with the nuclei of the air molecules, producing hadronic showers, cascades of many types of subatomic particles. Cosmic ray muons are the most numerous charged particles of these cascades, at sea level, and their energy and angular distribution at ground level [1] are the result of a convolution of the decay, the production spectrum, the energy loss in the atmosphere and the angular deviations due to collisions.

When a muon crosses a piece of material, it loses energy and is deflected from its original trajectory [2]. This phenomenon is stochastic and it is caused mainly by multiple scattering. The distribution of the deflection angle (θ) is described by the multiple scattering theory of Moliere [3]. For small deflection angles, less than 10°, it can be approximated by a Gaussian distribution, with mean value equal to zero [1].

Cosmic radiation has been known since the first decades of the 20th century: it has been considered for decades, the best source of projectiles to investigate the core of matter, from nuclei to elementary particles. Nowadays, cosmic rays are very important in Particle and Nuclear Physics, because they are used for detector testing and calibration, as described in [4–6], and for detector alignment in complex measurement apparatuses used in this field, like in [7–10], thanks to their high penetration capability. However, cosmic ray radiation has been already applied in fields beyond pure Physics. For instance, muon radiography has been used for geological research [11–14], archaeological studies [15] and it has been

 © 2007 IOP Publishing Ltd Printed in the UK

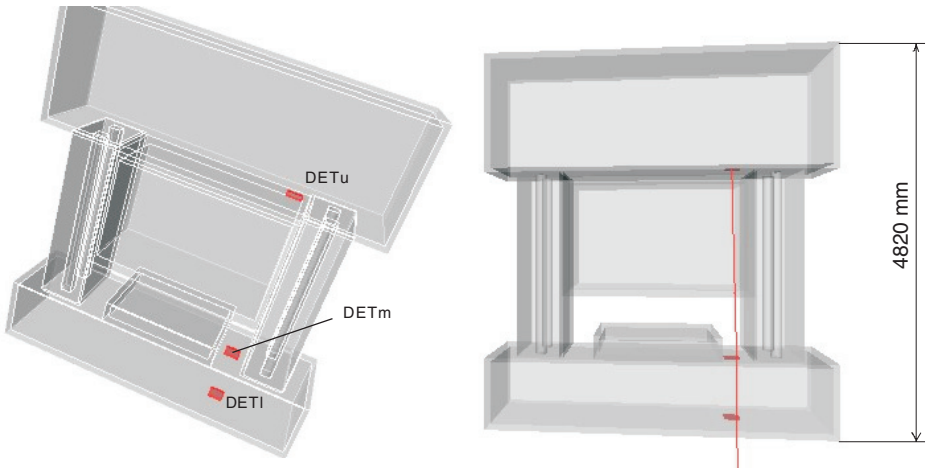

Figure 1. Pictures of the simulated configuration for the structure of the industrial press and the detectors, crossed by a cosmic ray. The upper (DETu), middle (DETm) and lower (DETl) detectors constitute the detection system, called telescope. They are mechanically connected to the parts of the structure whose relative positions have to be monitored.
(This figure is in colour only in the electronic version)

proposed to detect high-density materials in closed containers [16], especially to prevent contraband of radioactive material [17–19].

Due to their property of crossing very thick materials, cosmic rays appear as suitable tools for the realization of measurement systems, specially as a helpful alternative to traditional optical systems, when detectors are not mutually visible.

This paper is aimed at assessing potentialities and limits of muon detection techniques, when applied outside the field of Particle and Nuclear Physics, with particular reference to the engineering applications, such as alignment and positioning measurements and monitoring on large mechanical and civil structures. Advantages in the adoption of this methodology could be remarkable for several applications, i.e. where the parts to be measured are partially or completely inaccessible, making other conventional methods useless, where weakly controlled atmospheric conditions lessen the performances of traditional optical laser techniques [20] or where interposed materials prevent their use. A feasibility analysis performed by numerical simulations is proposed here, in order to verify the possible application of cosmic ray detection techniques to engineering measurements and monitoring problems. Moreover the results of this study could provide useful information to identify a specific detector to be used in such a measurement system.

2. Monte Carlo simulation of a reference case

The feasibility of a measurement system based on the detection of cosmic ray muons has been evaluated considering, as a representative example, the case of a mechanical press. The analysis has been performed by numerical simulations, with the aim of estimating the measurement uncertainty of the method and its dependence on the geometrical dimensions of the structure, on the materials interposed between the particle detectors, on the detector dimensions and spatial resolution and, ultimately, on the data-taking time.

The considered geometry is represented in figure 1. The press is about 5 m high, 1.5 m long and 1.2 m deep; the detection system (telescope) is mechanically connected to the parts of the structure that have to be monitored and is made up of three plane position detectors, placed in the upper (DETu), middle (DETm) and lower (DETl) parts of the press. The distance between DETu and DETl is 3.3 m, and the distance between DETu and DETm is 2.5 m; the detection plane of the simulated detectors is a sensitive 200 mm edge square and each detector is 10 mm thick. The simulated structure of the press is considered as composed of iron, whereas the volumes representing the detectors are made of plastic organic scintillator, a typical constituent of common particle detectors, such as scintillating fibres [2]. A more detailed simulation of a specific detector was not required since the results of the study are largely independent of the detector constituent material, with respect to the thickness of the crossed iron. In the simulation, the particle detectors are considered perfectly aligned on the vertical and each one is fixed to one of the components of the mechanical structure whose relative positions have to be monitored. As will be clear in the following, in a real system, this requirement would not be crucial and normal mechanical positioning precision is sufficient. A measurement system like the one described above shows the simplest realizable configuration, but it is an exhaustive example for what concerns the involved physical phenomena and the statistical analysis of the data.

The Monte Carlo simulations have been performed by a C++ toolkit for the simulation of the passage of particles through matter, called Geant4©: this package is largely used in Particle and Nuclear Physics studies [21]. The geometries of the press structure and of the detectors and their constituent materials have been taken into account in the simulations. The detector spatial resolution has been fixed to $\sigma = 100\ \mu$m on both coordinates of the sensitive surface, a typical value for different types of detectors. Finally, to obtain significant results, a realistic cosmic ray muon generator, based on experimental data [22], has been implemented in the code, in order to simulate, as realistically as possible, the momentum

and angular distributions of cosmic rays at the terrestrial surface.

3. Measurement of the detector alignment

The procedure to evaluate the detector alignment, implemented in the simulation and based on the measurement of the cosmic ray crossing points on the detectors, will be briefly described in the following.

When a cosmic ray crosses a detector, the coordinates of the hit are available. The response of each detector gives the position of the detection point in its horizontal sensitive plane. In the assumption of a muon straight line trajectory, the hits of the three detectors are aligned and a possible mechanical displacement of a particular detector of the telescope represents the systematic effect to be evaluated. However, the trajectory is a perfect straight line only in the absence of any magnetic field and when the muon crosses a vacuum. The interaction between the Earth's magnetic field and, for example, a 3 GeV/c momentum particle, causes a deflection of about 5 μm m^{-1} in the direction perpendicular to both magnetic field and particle velocity. Since in cosmic rays there is an excess of positive muons with respect to negative ones, this could induce a systematic effect on the measure. However, the proposed method is based on relative measurements, that is considering differences between measurements taken at different times, thus the effect of terrestrial magnetic field has been neglected in the following.

When a muon crosses any kind of matter, it deviates in a stochastic way, because of interactions, and the deviations are symmetrical around the flight path. The larger is the amount of the crossed matter, the more the stochastic effects are dominant, so a single cosmic ray is not, in general, sufficient to measure a possible systematic misalignment of a detector relative to the others. In addition, the spatial resolution of the detector is, in general, a source of uncertainty in the determination of the crossing point on the sensitive surface and it has random behaviour. A statistical distribution of the hit points of a population of cosmic rays crossing the detector telescope is therefore necessary, so stochastic effects on the position measurements can be reduced and treated by statistical inference methods. In this way, it becomes possible to extract information, from the data, about systematic effects, within a certain confidence level depending on the features of the distributions and the statistics of the collected sample.

To implement a procedure to analyse the data, two statistical variables, described in figure 2, have been defined: $\Delta x = x_{\rm int} - x_r$ and $\Delta z = z_{\rm int} - z_r$, where x and z are the two coordinates of the horizontal detection plane of the middle detector DETm (whereas y is the vertical direction of the adopted reference system). The two statistical variables are defined as the difference between the coordinate of the cosmic ray crossing point, detected by DETm, and the same coordinate of the intersection between the detection plane of DETm and the straight line connecting DETu and DETl cosmic ray hits.

The histograms of the variables Δx and Δz obtained with the full simulation are represented in figure 3; the mean values of these statistical distributions are connected to the systematic displacement of the middle detector relative to

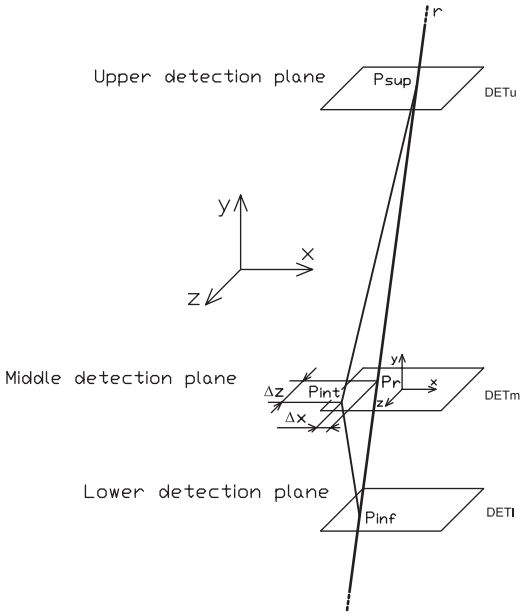

Figure 2. Δx and Δz are, respectively, the displacement along the x and z directions between the point $P_{\rm int}$, detected by the middle detector, and the intersection point P_r between the plane of the middle detector and the straight line that joins the hit points measured by the upper and the lower detectors. $\Delta x = x_{\rm int} - x_r$ and $\Delta z = z_{\rm int} - z_r$.

the others, in the two coordinates of the sensitive plane, while the standard deviation of each distribution is related to the uncertainty of the measurement of these systematic effects [23]. In the simulated geometry, detectors were perfectly aligned; therefore the two distributions are centred at zero. In effect, the proposed method is sensitive only to relative displacements among detectors and it is not possible to say which component has moved with respect to an absolute external reference system. Nevertheless, it can be effective to monitor variations of relative displacements of mechanical parts with time.

The rate of cosmic ray muons that reach the terrestrial surface is rather low and their angular distribution, peaked at the vertical, is rather large. Data-taking time is closely related to the collected statistics and, consequently, to the achievable uncertainty on the measurement of the systematic displacement. In the simulated geometrical conditions described above, the detector system acceptance, that is the ratio between the number of cosmic rays crossing all three detectors and the number of cosmic rays hitting at least the upper detector, is $(1.63 \pm 0.23) \times 10^{-3}$. This low value is due to the small solid angle covered by the telescope, by the spread of the cosmic ray angular distribution around the vertical and by the deviations of the cosmic rays due to the multiple scattering in the interposed materials.

In conclusion, only one or two cosmic rays in one thousand hitting the upper detector are useful for building the Δx and Δz statistical distributions; therefore, long data-taking times are in general needed for a significant application of the method, at least, in a geometry similar to the proposed one. For example, to collect a sample of 35 000 significant cosmic rays, it is necessary to wait for about 5 weeks.

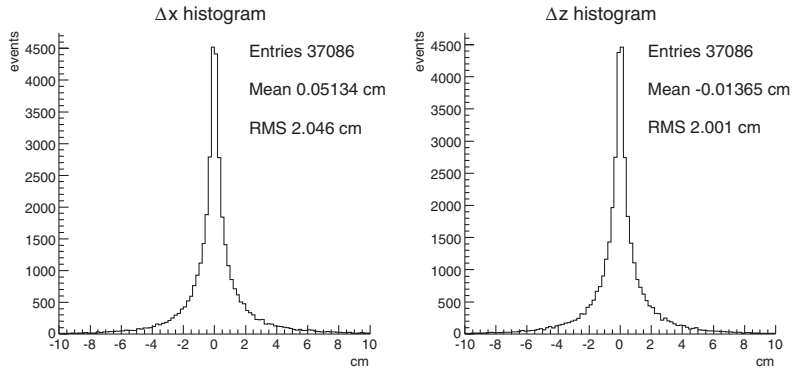

Figure 3. Histograms of the variables Δx and Δz for a large population of cosmic rays crossing the telescope.

4. Statistical analysis

4.1. Shape of the Δx and Δz parent populations

To perform an effective statistical analysis of the data, it is necessary to find efficient unbiased estimators that could return the values of both the possible displacement and of the uncertainty of its measurement. In order to find the best estimators, the shape of the distribution of the Δx and Δz parent populations, as seen in figure 3, has been approximated by a proper analytical function obtained by a best-fit procedure.

For a fixed value of the momentum of a particle, the physical process of the multiple scattering produces, at a first approximation, a Gaussian distribution of the deviation angle [1]. However, cosmic rays at the ground level have a wide momentum spectrum, and the material thickness that they have to cross may be different from one cosmic ray to another, because of the geometry of the structure, the different crossed thicknesses and the cosmic ray angular distribution. Therefore, the shape of the parent distributions of Δx and Δz is more complex than a simple Gaussian function. If the mechanical structure is symmetric enough, it is symmetrical around the vertical axis of the telescope and has long tails, due to the low momentum cosmic rays, which suffer larger deviations.

Since the main physical effect has Gaussian characteristics, at fixed particle momentum, it has been supposed that the distributions of figure 3 can be well represented by a sum of Gaussian functions with the same mean value and different standard deviations and weights. The number of Gaussian functions necessary to obtain a suitable best-fit function has been determined by fitting the distributions relative to figure 3 with sums of different numbers of Gaussian functions and by using statistical tests to determine the best number of functions. Proper statistical tests have also been used to verify the validity of the adopted form of the best-fit function.

The most general best-fit function is represented by the following formula:

$$f = \sum_{i=0}^{n-1} \frac{w_i}{\sigma_i} \mathrm{e}^{-\frac{1}{2}\left(\frac{t-m_i}{\sigma_i}\right)^2}. \qquad (4.1)$$

It depends on $3n$ parameters, where n is the number of Gaussian functions that compose the best-fit function: m_i are the mean values, σ_i are the standard deviations and w_i are the relative weights of each Gaussian function. Assuming that all the Gaussian functions have the same mean value ($m = m_i$), the number of free parameters decreases and becomes $(2n+1)$, i.e. n values both for σ_i and w_i and the common mean value m.

Two very large Monte Carlo samples, 43.0 and 21.5 millions of muons crossing the upper detector, have been generated, corresponding respectively to data-taking campaigns of about 2.50 and 1.25 months. They are used for producing high statistic distributions of Δz and Δx statistical variables, respectively, as seen in figure 4. The Δx distribution of the larger sample could not be used due to an excessive asymmetry caused by the presence of a pillar too close to the detector telescope, in the x direction, in that particular simulation. Indeed, in the simulation corresponding to the smaller sample, the detectors were placed at a larger distance from the pillar.

Fitting the obtained histograms of the statistical variables Δx and Δz with the most general best-fit function (4.1), the number of needed Gaussian functions (n), the value of the standard deviation (σ_i) and the relative weight (w_i) of each Gaussian function included in the sum have been determined and fixed, using the following statistical techniques: the least-squares method, the chi-square goodness-of-fit test and the F Fisher–Snedecor test for the evaluation of functional forms [24, 25].

In figure 4, the results of the fitting procedure are shown: for the Δx distribution five Gaussian functions were needed, whereas only four were needed for the more regular Δz distribution. The difference between Δx and Δz distributions is the consequence of a light asymmetry in the x direction of the press structure around the principal axis of the measurement telescope, caused by the presence of a pillar.

The resulting functions are a sum of Gaussian functions with the same mean value, fixed standard deviations and relative weights, and with only two free parameters: the common mean value (m) and a global scale coefficient (W). These functions represent the full population Δx and Δz and may be used to fit distributions of samples extracted from these. The best-fit parameter (m) constitutes an efficient estimator of the mean value of Δx and Δz populations. The standard deviation of the parameter m provides an estimation of the uncertainty in the measurement of the population mean value. This last parameter is directly dependent on the statistics of the sample.

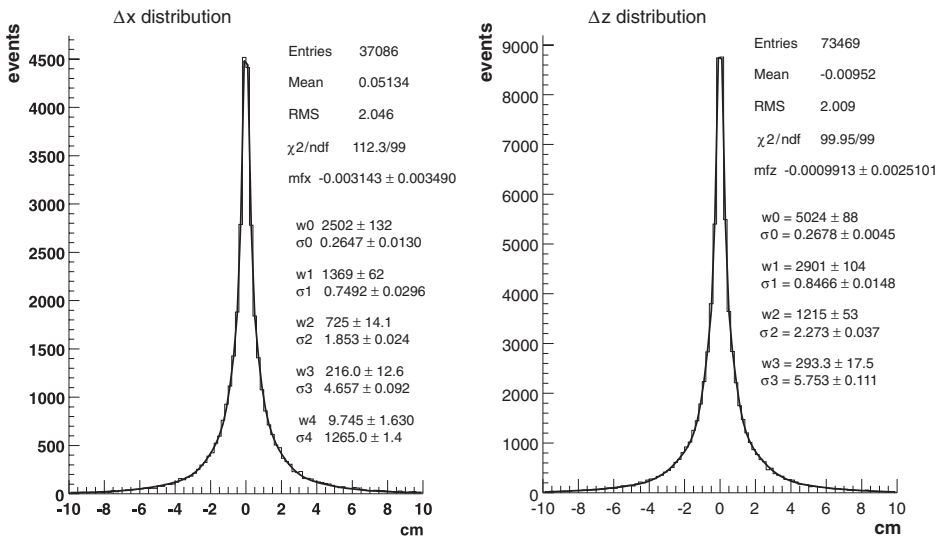

Figure 4. In these two figures the best-fit functions are superimposed on their respective Monte Carlo distributions for Δx and Δz statistical variables. Moreover the reduced χ^2 values, the best-fit function mean values (m_{f_x} and m_{f_z}) and the values of the (σ_i, w_i) parameters are reported.

Table 1. The table shows the comparison between the results obtained with the method based on the sample parameters and on the best-fit procedure.

			Sample quantities		Best-fit	
N_s (samples)	Generated muons	$\bar{N}_c$ (events)	ϵ_m (μm)	$\epsilon_{m'}$ (μm)	ϵ_{m_f} (μm)	ϵ_{s_f} (μm)
10	4 M	6848 ± 29	241.22 ± 56.86	242.77	86.31 ± 20.34	83.11 ± 0.29
21	2 M	3420 ± 14	384.56 ± 60.80	343.55	118.63 ± 18.76	118.60 ± 0.84
43	1 M	1790 ± 6	561.11 ± 61.22	486.03	192.22 ± 20.97	169.44 ± 1.45
86	500 k	854 ± 3	806.30 ± 61.84	687.35	255.24 ± 19.58	244.59 ± 1.89
172	250 k	427 ± 2	1025.66 ± 55.46	972.06	366.36 ± 19.81	347.26 ± 2.22
344	125 k	214 ± 1	1427.00 ± 54.50	1374.70	539.62 ± 20.60	483.00 ± 3.21

N_s = number of samples having the same generated number of events
$\bar{N}_c$ = average number of cosmic rays crossing the whole telescope, calculated on the N_s samples
ϵ_m = measurement uncertainty estimated by the standard deviation of the distribution of the N_s sample mean values
$\epsilon_{m'}$ = measurement uncertainty estimated by the ratio between the standard deviation of the whole population of 43 million generated events and the square root of $\bar{N}_c$
ϵ_{m_f} = measurement uncertainty estimated by the standard deviation of the distribution of the means (m) of the N_s best-fit functions
ϵ_{s_f} = measurement uncertainty estimated by the average of the errors in the mean values of the N_s best-fit functions calculated by error propagation in the fitting algorithm.

4.2. Relation between uncertainty and data-taking time

4.2.1. Data samples and estimators. The number of cosmic rays crossing the whole telescope is strictly connected to the data-taking time. To simulate periods of data taking of different length, the larger population of Monte Carlo data (43 millions of muons crossing the upper detector) has been split into smaller samples, characterized by different numbers of events. In particular, the following samples have been extracted:

10 samples of 4 M events, corresponding to a measurement time of 6.9 days per sample;

21 samples of 2 M events: measurement time 3.5 days per sample;

43 samples of 1 M events: measurement time 1.7 days per sample;

86 samples of 500 k events: measurement time 0.9 days per sample;

172 samples of 250 k events: measurement time 0.4 days per sample;

344 samples of 125 k events: measurement time 0.2 days per sample.

The evaluation of the measurement uncertainty of the telescope has been performed only on the Δz distribution, the procedure being the same for the Δx distribution. In this work, two methods have been used to obtain statistical estimators of the mean value of the parent population with their uncertainties, and the results have been compared. The first is simply based on the sample mean value and standard deviation of the distributions of the statistical variables; the second is based on the best-fit parameters returned by the aforementioned best-fit procedure, applied to the different samples. The results obtained by these two methods are reported and compared in table 1.

In table 1, the first column shows the number of samples into which the total population of 43 million events has been

split; the second one shows the number of generated muons in each sample of the corresponding row (muons crossing the upper detector); the third column shows the average number of muons crossing the whole telescope calculated over the corresponding samples; the fourth and fifth columns show the results for the measurement uncertainties obtained with the method of sample parameters and the sixth and seventh ones those obtained with the best-fit procedure.

In particular, in the fourth column, ϵ_m is the measurement uncertainty estimated by the standard deviation of the N_s sample mean values. In the fifth column, $\epsilon_{m'}$ is the measurement uncertainty estimated using the well-known relation for the error of the mean value of a sample, given by the ratio between the standard deviation of the parent population (relative to 43 million events generated) and the square root of the number of events in the sample. The compatibility between ϵ_m and $\epsilon_{m'}$ has been assessed checking that the value of $\epsilon_{m'}$ was included into the ϵ_m uncertainty interval, considering a 99.7% coverage interval. As expected, the estimated error in the mean value decreases with the number of events contained in the sample.

In the sixth column, ϵ_{m_f} is the measurement uncertainty estimated by the standard deviation of the distribution of the means (m) of the best-fit functions corresponding to the N_s samples. In the seventh column, ϵ_{s_f} is the measurement uncertainty estimated by the average value of the errors in the mean values of the N_s best-fit functions calculated by error propagation in the fitting algorithm. The compatibility between ϵ_{s_f} and ϵ_{m_f}, assessed by checking that ϵ_{s_f} was included into the ϵ_{m_f} uncertainty interval, demonstrates the statistical correctness of the fitting procedure.

The data in table 1 show that the best-fit procedure gives systematically better estimators, since, at the same value of $\bar{N}_c$, their uncertainties are smaller than the ones obtained by the sample parameters [23]. This result appears reasonable, since the best-fit procedure adds to the calculations extra information about the analytical shape of the parent population given as a continuous function obtained by the simulated parent distributions. Therefore, the construction and the use of the best-fit function of the parent population for fitting the sample distributions are justified.

In conclusion, to assess the measurement uncertainty of the displacement of a detector relative to the others, in the simulated configuration, by using a sample of cosmic rays containing N_c events, the value of ϵ_{s_f}, as defined in table 1, can be confidently adopted. For instance, for a sample of 1 million events, corresponding to a data taking of 1.7 days, the estimated uncertainty in the measurement of the systematic displacement of a detector is about 170 μm at one standard deviation. The measurement uncertainty depends on $\sqrt{N_c}$ as expected. This statement can be verified in the data in table 1 checking that the ratio between the uncertainty of a $\bar{N}_c$ sample and the uncertainty of a $2\bar{N}_c$ sample is $\sim\sqrt{2}$.

4.2.2. Uncertainty versus data-taking time. Cosmic ray flux at the terrestrial surface is about 1 cm^{-2} min^{-1}, so the number of generated muons reported in table 1 is directly proportional to the data-taking time (in realistic conditions, the muons crossing the upper simulated detector in a minute are about 400).

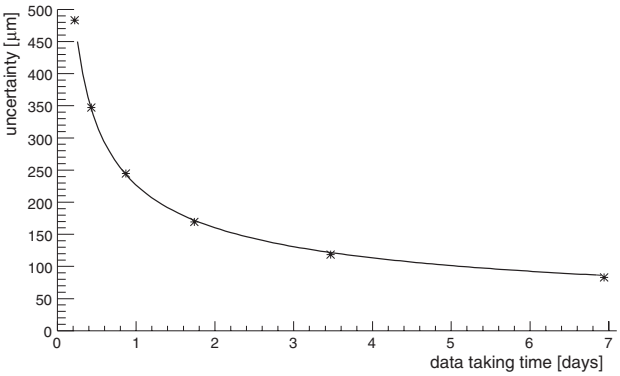

Figure 5. Relation between the average standard uncertainty of the measurement procedure and the data-taking time, up to a maximum of a week. The relation has been obtained using the ϵ_{s_f} column in table 1: the function in equation (4.2) has been fitted to the average standard uncertainties, obtaining (226.6 ± 0.3) μm day$^{1/2}$.

As aforementioned, the uncertainty relative to the measurement of the detector displacement depends on $\sqrt{\bar{N}_c}$; consequently it also depends on $\sqrt{t}$, where t is the data-taking time. Therefore, the general relation connecting the measurement uncertainty u and the data-taking time t can be written as

$$u = C \cdot t^{-1/2}, \tag{4.2}$$

where C is a constant, mainly depending on the system geometry and materials interposed between detectors.

In the considered conditions, using the values of the best estimators available in table 1 (i.e. the values of ϵ_{s_f}), it is possible to obtain the general relation between the average uncertainty of the measurement procedure and the data-taking time up to a week. This is done by fitting the function equation (4.2) on the values of ϵ_{s_f} reported in figure 5. The following best-fit function is obtained:

$$u = [(226.6 \pm 0.3)t^{-1/2}]\,\mu\text{m}, \tag{4.3}$$

where the data-taking time t is expressed in days, the constant is measured in μm day$^{1/2}$ and u is the standard uncertainty relative to the measurement procedure. As time increases, the uncertainty decreases and the relation (4.3) can be adopted as a general one representing the uncertainty of the measurement procedure for different data-taking times.

Equation (4.3) depends on the particular geometry of both the mechanical structure and the detector telescope, on the materials that cosmic ray muons have to cross and on their thickness and on the detector spatial resolution; therefore the whole procedure would have to be repeated if geometry and/or materials were modified.

4.2.3. Dependence of the uncertainty on other effects. As further studies, the effects of the interposed material thickness and composition and of the spatial resolution of the detectors on the measurement uncertainty of the telescope have been evaluated.

In particular, figure 6 shows the uncertainty as a function of the data-taking time for three different values of the thickness of the materials interposed between detectors, i.e. 900 mm, 280 mm and 120 mm of crossed iron. A lower

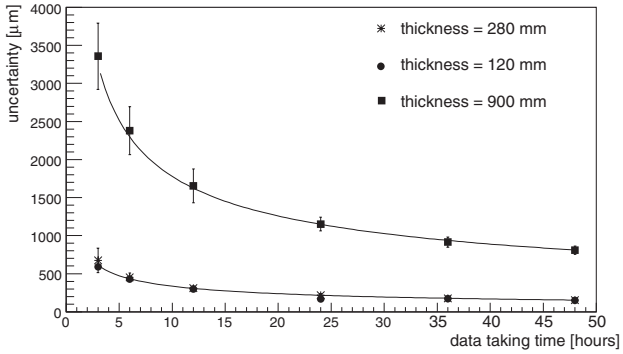

Figure 6. Comparison among the relations between measurement uncertainty and time, obtained changing the iron thickness crossed by cosmic rays between detectors. The thinner the crossed thickness, the less the obtained uncertainty.

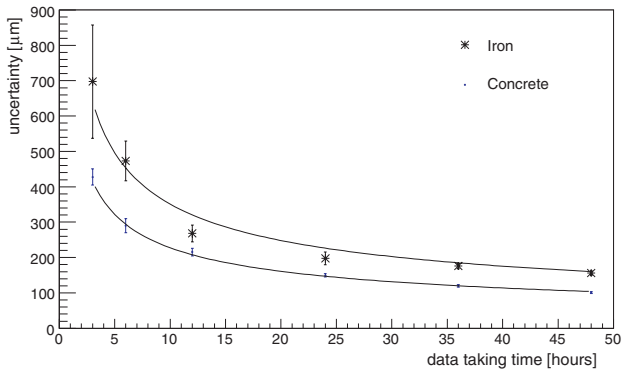

Figure 7. Measurement uncertainty versus time for concrete and iron: both are obtained on equal thickness, changing the crossed material. The less dense the material crossed by cosmic rays, the less the standard uncertainty of the measure.

uncertainty is obtained with less interposed material, but it may appear surprising that the functions relative to 280 mm and 120 mm of interposed material thickness appear superimposed.

In general, the thinner the crossed material thickness, the less the measurement uncertainty, since the effects generating cosmic ray deviations are less relevant. However, under certain conditions, a compensation takes place between the amount of multiple scattering and the modification of the momentum spectrum of the cosmic rays crossing the whole telescope, which depends on energy loss by ionization.

Indeed, in this specific case, when the crossed iron is at the minimum value of 120 mm thickness, the effect of multiple scattering is minimized, but a larger number of cosmic rays with very low momentum crosses the whole detector telescope, undergoing larger trajectory deviations. When the thickness of iron is increased to 280 mm, fewer cosmic rays cross the whole measurement system, a part of them being stopped in the interposed material, but they have more energy on average and suffer less deviation. The effects of this interplay can hardly be calculated analytically and a Monte Carlo simulation, which accounts accurately for the geometrical distribution of materials and the muon interactions with matter, is needed to obtain meaningful results.

Concerning the effect of different interposed materials on the measurement uncertainty, figure 7 shows a comparison between the relation of equation (4.2), calculated on equal thickness and geometry of iron and concrete. The latter is less dense than iron and generates less multiple scattering, thus allowing for better performance of the measurement system.

To understand how the detector spatial resolution influences the whole telescope measurement uncertainty, the simulations have been repeated for detectors having spatial resolution $\sigma = 100$ μm and $\sigma = 1.0$ mm; in particular, so far, all the evaluations have been performed adopting detectors having a spatial resolution $\sigma = 100$ μm. The result is that, in the simulated configuration, multiple scattering is the dominant effect affecting measurement uncertainty, and a degradation of the detector spatial resolution up to $\sigma = 1.0$ mm, which corresponds to a very coarse resolution, does not sensibly change the results.

5. Resolution of the measurement system for a mechanical misalignment

If a misalignment in the relative position of the detectors is imposed in the simulated geometry, a change of the calculated mean values of the sample distributions of the statistical variables Δx and Δz is expected; in contrast, if the displacement is sufficiently small, so that the solid angle covered by the detector telescope does not sensibly vary, no variation of the standard deviations of the sample distributions should result.

Figure 8 shows Δx and Δz histograms obtained by imposing, in the Monte Carlo simulation, a large displacement of the middle detector of the telescope, of $\Delta S_x = +2$ cm and $\Delta S_z = -2$ cm. The distributions are now centred around the value of the imposed displacement.

In a realistic measurement, since the detectors are positioned with a standard mechanical precision, the reference geometry of the system must be calibrated. With this aim, a 1 week long measurement campaign can be foreseen for the calibration of the system; for such a period a measurement standard uncertainty of about $\epsilon_0 = 85$ μm is expected in the measurement of the two reference positions (m_{0_x}, m_{0_z}) of the middle detector with respect to the other two, recalling that equation (4.3) determines the measurement uncertainty, at one standard deviation, for a sample of cosmic rays collected during a data-taking time t_i. To assess a possible positive displacement ΔS_x of the mechanical structure in the x direction, the following standardized variable is constructed:

$$s_x = \frac{\left(m_x^{t_i} - m_{0_x}\right) - \Delta S_x}{\sqrt{\epsilon_0^2 + \epsilon_{t_i}^2}} \tag{5.1}$$

where $m_x^{t_i}$ is the mean value of best-fit function applied to the Δx distribution of the sample collected in the data-taking time t_i, ϵ_{t_i} is the corresponding one standard deviation uncertainty, obtained from equation (4.3), the other symbols have the aforementioned meaning.

To assess the displacement ΔS_x at a 99.85% level of significance, with a 3σ test at one tail, the standardized variable s_x should be larger than -3. In order to exclude from the confidence interval of 3σ the reference value of the

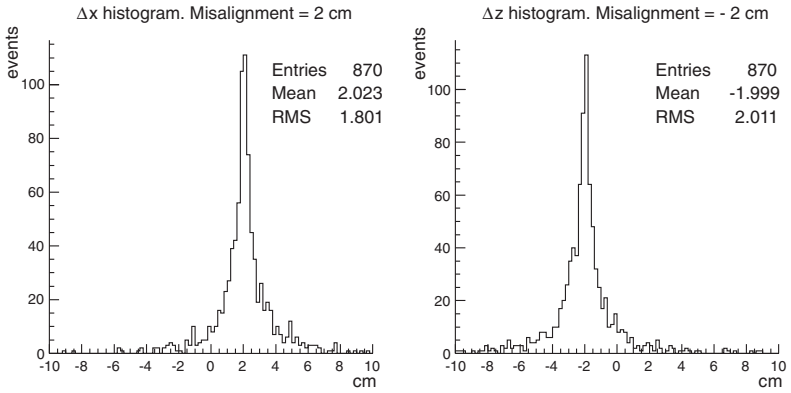

Figure 8. The Δx and Δz histograms after imposing a 2 cm displacement in both directions on the middle detector of the telescope. The sample standard deviations are statistically compatible with respect to the distribution represented in figure 3, but the mean values are displaced by an amount equal to the imposed displacement. The two distributions correspond to 21 h data taking.

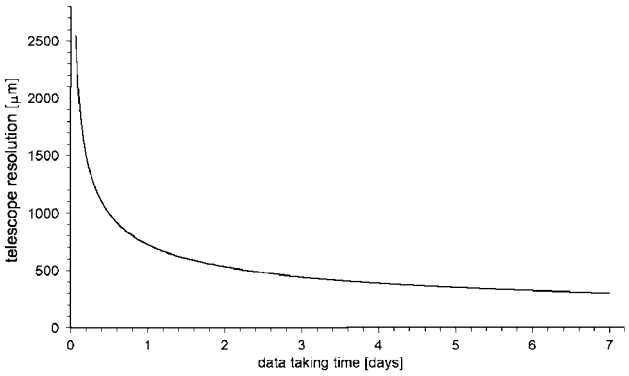

Figure 9. Resolution of the measurement system as a function of the data-taking time calculated for the considered geometry and supposing a calibration data taking of 1 week.

displacement m_{0x}, $\Delta S_x - 3\sqrt{\epsilon_0^2 + \epsilon_{t_i}^2}$ should be greater than zero and, consequently

$$\epsilon_{t_i} < \sqrt{\left(\frac{\Delta S_x}{3}\right)^2 - \epsilon_0^2} \tag{5.2}$$

This relation sets the maximum one standard deviation measurement uncertainty of the mean value of the best-fit function of the Δx distribution for assessing, within a 99.85% level of significance, a displacement ΔS_x of the middle detector. Equation (5.2) establishes also the relation between the resolution of the measurement system and the data-taking time, because the value of ϵ_{t_i} is related to the data-taking time.

Figure 9 shows this relation calculated in the considered geometry and supposing a calibration data taking of 1 week. One can see that the system is able to detect a relative displacement of 1.0 mm in about 12 h of measurement, whereas 60 h are needed to detect a 0.5 mm displacement. It is important to recall that these performances are obtained in a geometrical condition where the external detectors of the telescope, whose area is only 400 cm^2, are 3.3 m far away and the cosmic rays cross tens of centimetres of iron interposed between the detectors.

6. Summary and conclusions

Cosmic ray muon detection techniques for apparatus alignment are widespread in the field of Particle and Nuclear Physics. A feasibility analysis concerning possible applications of these methods in mechanical and civil engineering is proposed in this work.

Specifically, a preliminary study for the case of monitoring the alignment of an industrial press has been developed, performing Monte Carlo simulations. A telescope formed by three position detectors, vertically aligned, has been linked to the mechanical structure of the press. The position of the intermediate detector, relative to the other two, has been determined by measuring the hitting positions of cosmic rays crossing the whole telescope and performing an appropriate statistical analysis of data, based on the distributions of the two statistical variables Δx and Δz defined in section 3.

The position measurement standard uncertainty is the most significant considered parameter. It is directly connected to the data-taking time. The relation connecting the reachable standard uncertainty u and the data-taking time t is given by equation (4.2), where C is a parameter depending on the detector telescope features (detector size, distance between detectors, detector intrinsic resolution) and on the mechanical structure on which the telescope is placed (interposed materials and thicknesses, geometry).

For the studied configuration, where the distance between the most external detectors was 3.3 m and the total crossed iron thickness was 280 mm, $C = (226.6 \pm 0.3)\ \mu\text{m}\,\text{day}^{1/2}$. Standard uncertainty improves when the crossed thickness and/or interposed material density decrease. The sample distributions Δx and Δz must be fitted with best-fit functions representing the shapes of the parent population of the Δx and Δz statistical variables. The best-fit parameters of the fitting functions are correlated with the position measurement and its uncertainty.

The shapes of the parent populations are obtained by fitting a sum of Gaussian functions with the same mean value and different standard deviations and weights (see equation (4.1)) on a very large sample of data. Such very large samples, of the order of one hundred thousand cosmic rays crossing the whole telescope, are hardly obtained with a

real data taking that should last a very long time, of the order of 2.5 months for the considered geometry.

In this work, it is demonstrated that the simulation, by the Monte Carlo method, of any mechanical system on which measurement and monitoring techniques based on detection of cosmic rays should be applied, can be a valuable tool. It can be used to study the shapes of the Δx and Δz parent populations and obtain reliable best-fit functions, to optimize the position of the detector telescope relative to the mechanical structure and to determine, *a priori*, the relation between standard measurement uncertainty and data-taking time.

A possible improvement to the system is the use of an additional absorber below the third detector, followed by a fourth detector, e.g. a large plane scintillation counter. Requiring the coincidence of such a detector, the low-energy large multiple-scattering component of the included muons would be eliminated. For example, if a 300 mm iron absorber was placed under the press, which already accounts for 280 mm of iron, the coincidence with the fourth detector would eliminate all muons below 900 MeV/c, thus improving the system uncertainty. Of course, such an additional counter is not practical in all topologies, but where possible it could improve uncertainty and reduce data-taking time.

In the studied reference case, assuming a calibration time of 1 week data taking to set the reference position of the detectors, a displacement $\Delta S = 1.0$ mm is detectable by a measurement of about 12 h and a displacement $\Delta S = 0.5$ mm after a measurement time of 60 h, as shown in figure 9.

The most important factors affecting the performance of the system are the solid angle covered by the detector telescope and the amount of multiple scattering suffered by cosmic ray muons crossing the telescope. Detector intrinsic spatial resolution seems not to be a crucial parameter.

The studied measurement method is suitable to detect relative displacements among parts of the same structure, both translations and rotations; so it could be particularly useful when the purpose is monitoring the relative positions of parts of a structure with time. Moreover, using more than three detectors in the telescope, it could be possible to produce also an image of the deformed structure.

This method could be particularly useful when the parts that have to be monitored are not reciprocally visible or when the measuring area is hardly accessible directly. The distances between two successive detectors do not represent a restriction for the reachable uncertainty that just depends on the data-taking time available. The last is the most limiting factor of the method.

Different potential applications of this method can be found both in civil and industrial engineering.

(i) *Civil engineering field*. Installations to supervise static stability of (a) dams, in place of the current expensive inverse-pendulum; (b) historical monuments, such as towers and belfries; and (c) constructions in seismic-risk areas. The advantages could be a low upkeep and steady data acquisition. The last would permit data to be collected continuously and increase available statistics. The cosmic ray detection based method shows reachable uncertainties which are comparable to those affecting other monitoring systems typically used in this field, such as laser scanner and theodolites [26, 27], global positioning system based methods [28] or pendulums [29].

(ii) *Industrial engineering and big structures field*. Installations to monitor structural degradation, i.e. permanent deformations of big structures such as construction site and shipyard cranes, big presses, dock and airport hulls [16]. The measurement uncertainties obtained by this method are comparable with the industrial traditional ones, such as electronic levels or laser alignment [30, 31] and with interferometric laser techniques [29, 32], if they are employed in weakly controlled conditions [20].

References

[1] Review of Particle Physics 2000 *Eur. Phys. J.* C **15** 1
[2] Leo W R 1994 *Techniques for Nuclear and Particles Physics Experiments—A How-to Approach* 2nd revised edn (Berlin: Springer)
[3] Bethe H A 1953 *Phys. Rev.* **89** 1256
[4] Bertl W *et al* 2005 *Eur. Phys. J.* C **41** 11
[5] Aguilar-Benítez M *et al* 2002 *Nucl. Instrum. Methods* A **480** 658
[6] Bianchini P *et al* 2006 *IEEE Trans. Nucl. Sci.* **53** 317
[7] Benettoni M *et al* 2004 Study of the internal alignment of the CMS muon barrel drift chambers using cosmic ray tracks *CMS Note* 2004/001 http://cmsdoc.cern.ch/documents.html
[8] Piano S 2001-2002 Search for sigma hypernuclear states with the FINUDA spectrometer *PhD Thesis* Trieste University. http://www.ts.infn.it/experiments/finuda/piano_phd.pdf
[9] Tomassini S, Ceccarelli A and Di Virgilio A 2001 FINUDA silicon vertex detector measurement *FINUDA Internal Technical Note*
[10] Agnello M *et al* 2000 *Performances of the FINUDA drift chambers in a cosmic ray test* LFN-00/030 (IR). http://www.lnf.infn.it/sis/preprint/
[11] Georges E P 1955 *Commonwealth Engineer* p 455
[12] Caffau E, Coren F and Giannini G 1997 *Nucl. Instrum. Methods* A **385** 480
[13] Nagamine K *et al* 1995 *Nucl. Instrum. Methods* A **356** 585
[14] Tanaka H *et al* 2003 *Nucl. Instrum. Methods* A **507** 657
[15] Alvarez L W *et al* 1970 *Science* **167** 832
[16] Janneson P M 2004 *Nucl. Instrum. Methods* A **525** 346
[17] Schultz L J 2003 Cosmic ray muon radiography *PhD Thesis* Portland State University
[18] Priedhorsky *et al* 2003 *Rev. Sci. Instrum.* **74** 4294
[19] Gustafsson J 2005 Tomography of canister for spent nuclear fuel using cosmic-ray muons *Diploma Thesis* Uppsala University Neutron Physics Report http://www.inf.uu.se/Reports/UUNF05-08.pdf
[20] Magalini A and Vetturi D 2006 Laser interferometry for straightness in a weakly controlled environment *XVIII IMEKO World Congress Proc.—Metrology for a Sustainable Development (Rio de Janeiro, Brazil)*
[21] Geant4 collaboration 2003 *Nucl. Instrum. Methods* A **506** 250
[22] Kremer J *et al* 1999 *Phys. Rev. Lett.* **83** 4241
[23] BIPM, IEC, IFCC, ISO, IUPAC, IUPAP and OIML 2004 *Guide to the Expression of Uncertainty in Measurement Supplement 1: Numerical Methods for the Propagation of Distributions* (Draft version) (Geneva: ISO)
[24] Rotondi A, Pedroni P and Pietavolo A 2005 *Probabilità Statistica e Simulazione* (Milan: Springer-Verlag Italia)
[25] Vicario G and Levi R 1998 *Calcolo Delle Probabilità per Ingegneri* (Bologna: Progetto Leonardo)
[26] Alba M *et al* 2006 Structural monitoring of large dam by terrestrial laser scanning *Proc. ISPRS Commission V Symp.—Image Engineering and Vision Metrology vol 36 (Dresden, Germany)*
[27] *Leica industrial theodolites and total stations—highest industrial precision* Leica industrial theodolites and total stations data-sheet

[28] Website of the School of Surveying and Spatial Information Systems, University of South New Wales (Sydney, Australia) http://www.gmat.unsw.edu.au/snap/gps/gps_survey/chap10/chap10.htm
[29] Doeblin E O 1990 *Measurement Systems—Application and Design* (New York: MacGraw-Hill International Editions)
[30] Tesa Niveltronic data-sheet http://www.tesach.ch/catalog/
[31] Leuze Electonic data-sheet http://www.leuze.com/products/products_en.html
[32] Laser measurement system LSP Compact data-sheet http://www.feanor.com/